Heterozygous Mutations in *OAS1* Cause Infantile-onset Pulmonary Alveolar Proteinosis with Hypogammaglobulinemia

Running head: Alveolar proteinosis with hypogammaglobulinemia

Kazutoshi Cho,[1,10,*] Masafumi Yamada,[2,10] Kazunaga Agematsu,[3] Hirokazu Kanegane,[4] Noriko Miyake,[5] Masahiro Ueki,[2] Takuma Akimoto,[1] Norimoto Kobayashi,[3] Satoru Ikemoto,[6] Mishie Tanino,[7] Atsushi Fujita,[5] Itaru Hayasaka,[1] Satoshi Miyamoto,[4] Mari Tanaka-Kubota,[4] Koh Nakata,[8] Masaaki Shiina,[9] Kazuhiro Ogata,[9] Hisanori Minakami,[1] Naomichi Matsumoto,[5] and Tadashi Ariga[2]

[1]Maternity and Perinatal Care Center, Hokkaido University Hospital, Sapporo, 060-8648, Japan; [2]Department of Pediatrics, Faculty of Medicine and Graduate School of Medicine, Hokkaido University, Sapporo, 060-8638, Japan; [3]Department of Pediatrics, Shinshu University, School of Medicine, Nagano, 390-8621, Japan; [4]Department of Pediatrics and Developmental Biology, Tokyo Medical and

Dental University, Tokyo, 113-8519, Japan; [5]Department of Human Genetics, Yokohama City University Graduate School of Medicine, Yokohama, 236-0004, Japan; [6]Division of General Pediatrics, Saitama Children's Medical Center, Saitama, 330-8777, Japan; [7]Department of Cancer Pathology, Faculty of Medicine and Graduate School of Medicine, Hokkaido University, Sapporo, 060-8638, Japan; [8]Bioscience Medical Research Center, Niigata University Medical & Dental Hospital, Niigata, 951-8520, Japan; [9]Department of Biochemistry, Yokohama City University Graduate School of Medicine, Yokohama, 236-0004, Japan

[10]These authors contributed equally to this work.

*Correspondence: chotarou@med.hokudai.ac.jp

Abstract

Pulmonary alveolar proteinosis (PAP) is characterized by accumulation of a surfactant-like substance in alveolar spaces and hypoxemic respiratory failure. Genetic PAP (GPAP) is caused by mutations in genes encoding surfactant proteins, or genes encoding a surfactant phospholipid transporter in alveolar type II epithelial cells. GPAP is also caused by mutations in genes that could be responsible for surfactant catabolism in alveolar macrophages (AMs). We performed whole exome sequence analysis in a family affected by infantile-onset PAP with hypogammaglobulinemia without mutations in known causative genes. The same heterozygous missense variation in *OAS1*, encoding 2',5'-oligoadenylate synthetase 1 (OAS1), was identified in three affected siblings but not in unaffected family members. Deep sequence analysis with next-generation sequencing indicated 3.81% mosaicism of this variation in DNA from their mother's peripheral blood leukocytes, suggesting that PAP observed in this family could be inherited as an autosomal dominant trait from the mother. We identified two additional *de novo* heterozygous missense variations of *OAS1* in two unrelated sporadic

affected individuals also manifesting infantile-onset PAP with hypogammaglobulinemia. PAP in the two sporadic affected individuals resolved after hematopoietic stem cell transplantation, indicating that OAS1 dysfunction was associated with impaired surfactant catabolism due to the defects in AMs.

Lung surfactant is synthesized and stored in alveolar type II epithelial cells.[1] It is secreted into the alveolar spaces and reduces surface tension at air–liquid interfaces. Surfactant proteins (SP)-B and SP-C are highly hydrophobic and essential for the surface activity of lung surfactant.[2] ATP-binding cassette A3 (ABCA3) transports surfactant phospholipids into lamellar bodies where they bind SP-B and SP-C to form surfactant.[3] Secreted lung surfactant is partially recycled by type II epithelial cells, and the remainder is taken up and catabolized by alveolar macrophages (AMs). Granulocyte-macrophage colony-stimulating factor (GM-CSF) is implicated to be essential for catabolism of lung surfactant, as well as the proliferation and maturation of human AMs.[4]

Pulmonary alveolar proteinosis (PAP) is caused by lung surfactant system homeostasis dysfunction.[5] PAP can be categorized into four types: autoimmune PAP (APAP) (MIM 610910), secondary PAP (SPAP), genetic PAP (GPAP), and unclassified PAP. APAP is caused by excess production of autoantibodies against GM-CSF.[6] AMs of APAP individuals show a typical foamy appearance.[7] SPAP is associated with underlying malignancies or blood diseases, such as myelodysplastic syndrome (MIM

614286).[8] GPAP is caused by mutations in various genes.[9,10] SP-B, encoded by one of the genes responsible for GPAP, *SFTPB* (MIM 178640), is required for the maturation of SP-C. SP-B deficiency (MIM 265120) is an autosomal recessive disease characterized by respiratory distress syndrome (RDS) (MIM 267450) at birth, which then develops into infantile type PAP.[11] Abnormalities in SP-C (encoded by *SFTPC* [MIM 178620]) (MIM 610913) and ABCA3 (encoded by *ABCA3* [MIM 601615]) (MIM 610921) are likely to yield manifestations of GPAP and interstitial pneumonitis.[12,13,14] Mutations in genes encoding GM-CSF receptor (*CSF2RA* [MIM 306250] and *CSF2RB* [MIM 138981]) are also associated with GPAP (MIM 300770) (MIM 614370) in infants and adults.[15,16,17] Mutations in *GATA2* (MIM 137295) are associated with monocytopenia and mycobacterial infection (MonoMAC) syndrome (MIM 614172), which shows a broad spectrum of clinical manifestations, including PAP.[18]

In this study, we performed whole exome sequence (WES) analysis in a family affected by infantile-onset PAP with hypogammaglobulinemia that had no mutations in known causative genes: *SFTPB*, *SFTPC*, *ABCA3*, *CSF2RA*, *CSF2RB*, and

GATA2. In addition, we further studied two unrelated sporadic affected individuals that also presented with infantile-onset PAP with hypogammaglobulinemia. A summary and details of the affected individuals are shown in Table 1 and Supplemental Data, respectively.

This study was conducted in accordance with the Declaration of Helsinki and the national ethical guidelines, and was approved by the Ethics Committees of Hokkaido University Faculty of Medicine and Graduate School of Medicine (16-001), Yokohama City University Graduate School of Medicine, and Tokyo Medical and Dental University. Parents of all individuals included in the study provided written informed consent for genetic analyses and publication. The genomic DNA of the first (A-II-1) and third (A-II-3) affected siblings in family A had been extracted by phenol/chloroform methods and stored at –80°C (Figure S1A). The genomic DNA samples of other family members were extracted from heparinized peripheral blood samples using SepaGene (Sankojunyaku, Tokyo, Japan). All DNA samples were amplified with an Illustra GenomiPhi DNA Amplification Kit (GE Healthcare, Little Chalfont, UK). In addition, we established Epstein-Barr virus-transformed

lymphoblastoid cell lines (EBV-LCL) from the patient (A-II-4) and her unaffected sibling (A-II-2) and also extracted their DNAs. WES analysis was performed as described previously.[19] Briefly, 3 μg of whole genome amplified DNA from peripheral blood or DNA samples from EBV-LCL were used in sample preparation. Genome partitioning was performed with SureSelect Human All Human Exon v4 (Agilent Technology, Santa Clara, CA) according to the manufacturer's protocol. The samples were run on a HiSeq2000 (Illumina, San Diego, CA) with 101-bp paired-end reads and 7-bp index reads. Reads were mapped to the human reference genome (GRCh37.1/hg19) by Novoalign 2.08.02. Variants were called with Genome Analysis Toolkit v1.6-5 and annotated using ANNOVAR (2012feb).

To identify the causative variants, we selected variants based on the following criteria. For the autosomal dominant (*de novo*) model, we first removed synonymous variants and then selected 1) variants not found in our in-house exome data (n = 153 controls), 2) variants not registered in dbSNP 135 (see Web Resources) or NHLBI Exome Sequencing Project (ESP5400) (see Web Resources), 3) variants outside segmental duplication, 4) variants not observed in either parents or an unaffected

sibling, and 5) variants shared among all three affected children. For the homozygous model, we first removed synonymous variants and then selected 1) rare variants ($n \leq$ 1/153) in our in-house exome data, 2) variants with minor allele frequency (MAF) $\leq$ 0.01 in ESP5400, 3) variants outside segmental duplication, and 4) variants shared in three affected children. For autosomal compound heterozygous variants, we first removed synonymous variants and then selected 1) rare variants ($n \leq 1/153$) in our in-house exome data, 2) variants with MAF ≤ 0.01 in ESP5400, 3) variants outside segmental duplication, and 4) variants shared among three affected children. To estimate the mosaic variation in their parents, we counted the reads with variation using the BAM file with Integrative Genomic Viewer (see Web Resources). To confirm the presence of the variant allele in peripheral blood, we sequenced the 151-bp amplicon covering the candidate *OAS1* (MIM 164350) variant by deep sequence analysis using MiSeq with Miseq Reagent Kit v1 (300 cycles) (Illumina). Genomic DNA samples from two unrelated sporadic affected individuals from families B and C (B-II-1 and C-II-1) (Figures S1B and S1C) were subjected to PCR amplification of the *OAS1* gene with primers to cover three transcriptional variants sharing the same exons 1 to 4

(RefSeq accession numbers NM_016816.3, NM_002534.3, and NM_001032409.2) as listed in Table S1. Direct sequence analysis of *OAS1* was performed as described previously.[20] Nucleotide sequences were compared with the reported reference sequence of *OAS1* (RefSeq NM_016816.3).

The free energy changes associated with each variation were calculated using FoldX software through the YASARA interface.[21] Crystal structures of the dsRNA-bound form of human 2',5'-oligoadenylate synthetase 1 (OAS1) (hOAS1) (PDB code 4ig8) and the apo form of pOAS1 (PDB code 1px5) were used for the calculation. After energy minimization with the "Repair object" command, free energy change upon each variation was calculated with the "Mutate residue" command through the YASARA interface.

The quality of WES performance is summarized in Table S2. The exonic regions were not well covered using the whole genome amplified samples (64.6%–89.6% of coding sequences by ≥ 20× reads). Although we first considered that the condition in family A was inherited in an autosomal recessive manner, there were no causative recessive variants (Tables S3 and S4). Unexpectedly, one *de novo* amino acid

substitution of c.227C>T, p.Ala76Val in *OAS1* (RefSeq NM_016816.3) was shared by all three affected individuals but not by unaffected family members (Figure 1A and Table S5). This variant was not registered in the ESP5400, Exome Aggregation Consortium (see Web Resources), or Human Genetic Variation Database (see Web Resources), and was predicted to be "Tolerated" by SIFT (see Web Resources) and "Polymorphism" by MutationTaster (see Web Resources), but "Probably damaging" by PolyPhen-2 (see Web Resources) (Table 2). This amino acid is evolutionarily conserved from opossum to human (Figure 2A) and is located between the metal binding sites (p.Asp75 and p.Asp77) in the NTP_transf_2 domain (Figure 2B). Biological parentage was confirmed based on nine microsatellite markers. As either of the parents could have this variant as a mosaic, we performed deep sequencing of the parents' amplicons covering this variant and detected the mutant T allele at a frequency of 3.81% in the mother (Table S6).

Furthermore, we found two additional heterozygous *OAS1* variants occurring *de novo* in two unrelated sporadic affected individuals with infantile-onset PAP with hypogammaglobulinemia (B-II-1 and C-II-1) (Figures S1B and S1C). A variation of

c.326G>A, p.Cys109Tyr in *OAS1* (RefSeq NM_016816.3) was observed in B-II-1, but not in her parents (Figure 1B). This missense variation was “Tolerated” by SIFT and “Polymorphism” by MutationTaster, but “Possibly damaging” by PolyPhen-2 (Table 2). Another variation of c.592C>G, p.Leu198Val in *OAS1* (RefSeq NM_016816.3) observed in C-II-1 but not in her parents (Figure 1C) was predicted as “Tolerated” by SIFT, “Benign” by PolyPhen-2, and “Polymorphism” by MutationTaster (Table 2).

To assess the impact of the identified variations of p.Ala76Val, p.Cys109Tyr, and p.Leu198Val on protein structure, we mapped these variations onto the crystal structures of a double-stranded RNA (dsRNA)-bound form of human OAS1 (hOAS1) and an apo form of porcine oligoadenylate synthetase 1 (pOAS1) (PDB codes 4ig8 and 1px5, respectively)[22,23] (Figure 3A). We also calculated the free energy change associated with each variation using FoldX software (Figure 3B). The conformation of OAS1 is stabilized in a catalytically active form, which is capable of binding to ATP and Mg^{2+} ions upon binding to dsRNA.[24] There are structural differences between the RNA-bound and apo forms (Figure 3A). p.Ala76 in hOAS1 (p.Ala75 in pOAS1) adjoins the two active site aspartic acid residues, p.Asp75 and p.Asp77 (p.Asp74 and

p.Asp76 in pOAS1), which bind to Mg^{2+} ions. The side chain of p.Ala76 is involved in a hydrophobic core that would define the active site structure in the RNA-bound form, indicating that the p.Ala76Val variation would affect the enzymatic activity. The side chain of p.Cys109 in hOAS1 (p.Cys108 in pOAS1) is involved in a hydrophobic core of the apo form of OAS1, which is rearranged upon dsRNA binding. There are structural differences around the cysteine residue between the RNA-bound and apo forms (Figure 3A). The FoldX calculation showed a marked increase in free energy associated with the p.Cys109Tyr variation in hOAS1 (p.Cys108Tyr in pOAS1) in the apo form of OAS1. This result suggested that the p.Cys109Tyr variation is likely to disrupt the hydrophobic core of the apo form and the importance of this residue for regulation of enzymatic activity by dsRNA. p.Leu198 in hOAS1 (p.Leu197 in pOAS1) is involved in a hydrophobic core, which is located close to the ATP binding pocket (Figure 3A). Thus, the p.Leu198Val variation in hOAS1 (p.Leu197Val in pOAS1) may impair ATP binding and enzymatic activity, although FoldX predicted only a small impact of p.Leu198Val on protein folding (Figure 3B). Neither p.Cys109Tyr nor p.Leu198Val variant in *OAS1* was registered in ESP5400, Exome Aggregation Consortium, or

Human Genetic Variation Database.

The mechanisms by which the heterozygous mutations of *OAS1* described above cause PAP are unknown, and functional studies are currently underway. The OAS1 protein, encoded by *OAS1*, is a member of the 2-5A synthetase family essential for innate immune response against viral infection.[25,26,27] OASs are induced by interferons and use adenosine triphosphate in 2'-specific nucleotidyl transfer reactions to synthesize 2',5'-oligoadenylates. These molecules activate latent RNase L, which results in degradation of both viral and endogenous RNA. In addition to antiviral activity, the OASs were reported to be involved in fundamental cellular functions, such as cell growth and differentiation, gene regulation, and apoptosis.[28] A single nucleotide polymorphism (SNP), rs10774671, causing *OAS1* splicing variant was shown to be associated with increased susceptibility to plasma leakage and shock in individuals infected with dengue virus-2, indicating that immune overreaction could be triggered by the specific *OAS1* genotype, at least in dengue virus infection.[29] Although the functions of OAS1 on AMs have not been fully elucidated, expression of OAS1 in AMs could be induced by oxidative stress.[30] The association of the G-allele of non-synonymous A/G

SNP in exon 3 and SNP in the 3'-untranslated region of *OAS1* with severe acute respiratory syndrome (SARS) susceptibility suggested the immune modulating function of OAS1 protein, especially in the respiratory system.[26, 27] Therefore, we speculated that the heterozygous mutations of *OAS1* observed in the three families, presumably gain-of-function mutations, may be associated with exaggerated immune reaction especially in AMs in response to viral infections, leading to dysfunction of AMs and impaired catabolism of lung surfactant.

There are a number of possible characteristic features of this disease, including infantile onset. All affected individuals were term infants and had no respiratory symptoms at birth. The onsets of respiratory symptoms were distributed from 39 days to 5 months. The first symptoms appeared like a viral infection in most of the individuals, including C-II-1, who was positive for respiratory syncytial virus (RSV), cytomegalovirus, and subsequently coronavirus NL63 in sputum specimens during onset. Viral infections may trigger the onset of PAP via the mechanisms proposed above.

Hypogammaglobulinemia was observed in three affected individuals (A-II-4,

B-II-1, and C-II-1), and was unclear in two individuals that died at 91 days (A-II-1) and 163 days (A-II-3). Three individuals that survived beyond the first year of life (A-II-4, B-II-1, and C-II-1) showed low levels of serum IgG, IgM, and IgA, although they had no B cell deficiency. Although the level of endogenous IgG was unknown due to repeated intravenous immunoglobulin (IVIG) administration, serum IgM and IgA levels increased gradually during the course of the disease. Hypogammaglobulinemia observed in affected individuals may be due to impaired B cell function by an as yet unknown mechanism caused by heterozygous *OAS1* mutations.

Small and non-foamy AMs were observed in four affected individuals (A-II-1, A-II-3, A-II-4, and C-II-1) and were undetermined in one individual (B-II-1). In contrast with the large and foamy AMs observed in APAP,[31] small and non-foamy AMs may indicate dysfunction of maturation and/or phagocytosis of AMs rather than impaired catabolism of phagocytosed lung surfactant. Although we performed BAL four times in A-II-4 and there were many CD14-positive small and non-foamy AMs every time, this finding was based on a single bronchoalveolar cell cytopathology specimen showing less than 20 cells in most of the individuals. Further studies in larger

numbers of affected individuals with this disease are necessary.

Three patients (A-II-4, B-II-1, and C-II-1) had overwhelming inflammation, which was not clear but was confirmed at autopsy in two patients (A-II-1 and A-II-3). Splenomegaly, possibly related to hyperinflammation, was observed in four patients (A-II-1, A-II-3, A-II-4, and C-II-1) before the initiation of replacement therapy with IVIG. Exogenous IgG improved respiratory symptoms and decreased systemic inflammatory responses in A-II-4, B-II-1, and C-II-1. However, AMs in bronchoalveolar lavage (BAL) fluid from A-II-4 under sequential IVIG showed no improvement in viability or phagocytosis of AMs (data not shown). Furthermore, A-II-4 showed gradual progression of PAP. Thus, immunoglobulin administration may be able to suppress uncontrolled inflammatory responses, without being able to improve dysfunction of AMs in terms of surfactant phagocytosis or catabolism. As inflammation plays an important role in the pathophysiology of PAP,[32] immunomodulation by IVIG may have some effect on the clinical course of PAP.

B-II-1 died from renal failure due to glomerulosclerosis following hematopoietic stem cell transplantation (HSCT). Glomerular diseases, including

glomerulosclerosis, are increasingly observed especially in individuals with graft versus host disease after HSCT.[33] As renal biopsy was performed at the end stage of renal failure, it was difficult to determine whether glomerulosclerosis observed in B-II-1 was associated with HSCT. As another affected individual, A-II-4, showed proteinuria before initiation of monthly IVIG, OAS1 dysfunction itself could cause glomerular diseases. Long-term observation and accumulation of more individuals with this disease are necessary to evaluate this association.

Lung transplantation is a curative treatment for GPAP caused by mutations in genes encoding surfactant proteins, or genes encoding a surfactant phospholipid transporter in alveolar type II epithelial cells.[34] On the other hand, HSCT is effective for GPAP caused by mutations in genes that could be responsible for surfactant catabolism in AMs.[35] In this study, two affected individuals (B-II-1 and C-II-1) received successful HSCT and recovered completely from PAP. C-II-1 has had cord blood engraftment for 2 years without any respiratory symptoms. It has been reported that AMs are derived from precursor cells in bone marrow.[36] Pulmonary transplantation of differentiated wild-type AMs derived from bone marrow in GM-CSF receptor-β-deficient mice

showed long-term effectiveness due to proliferation of transplanted AMs.[37] Although IVIG could transiently improve the clinical condition, HSCT is the most effective therapy for this disease at present.

In summary, heterozygous mutations in *OAS1* cause infantile-onset PAP with hypogammaglobulinemia possibly caused by dysfunction of AMs. Infantile onset, leukocytosis without abnormal distribution, splenomegaly, and hyperreactivity were the most prominent findings. HSCT should be considered a curative treatment for this disease.

Acknowledgments

Professor JA Whitsett and Dr. W Hull (Cincinnati Children's Hospital Medical Center, Cincinnati, OH) performed Western blotting of SP-B in Case A-3 and measured concentrations of SP-A and SP-B in Case A-3, respectively. Professor H Hasegawa (Tokyo Women's Medical University Medical Center East) supported BAL examination of Case C-II-1.

Statement of Financial Support

This study was supported by grants for: “Practical Research Project for Rare/Intractable Diseases” from the Japan Agency for Medical Research and Development; Research on Measures for Intractable Diseases; Comprehensive Research on Disability Health and Welfare, the Strategic Research Program for Brain Science; Initiative on Rare and Undiagnosed Diseases in Pediatrics and Initiative on Rare and Undiagnosed Diseases for Adults from the Japan Agency for Medical Research and Development; Grants-in-Aid for Scientific Research on Innovative Areas (Transcription Cycle) from the Ministry of Education, Science, Sports, and Culture of Japan; Grants-in-Aid for Scientific Research (B) from the Japan Society for the Promotion of Science; Creation of Innovation Centers for Advanced Interdisciplinary Research Areas Program in the Project for Developing Innovation Systems from the Japan Science and Technology Agency; grants from Ministry of Health, Labor and Welfare; the Takeda Science Foundation; the Yokohama Foundation for Advancement of Medical Science; and the Hayashi Memorial Foundation for Female Natural Scientists.

Disclosure:

None of the authors have any conflicts of interest to disclose.

Figure Legends

Figure 1. *OAS1* variations in three families with PAP

Genetic analysis for *OAS1* variation. Sanger sequencing demonstrated variations of (A) c.227C>T, p.Ala76Val in family A, (B) c.326G>A, p.Cys109Tyr in family B, and (C) c.592C>G, p.Leu198Val in family C. Black arrows show the positions of the variations.

Figure 2. Evolutionary conservation and variations in *OAS1*

(A) Evolutionary conservation of p.Ala76, p.Cys109, and p.Leu198 amino acids in human OAS1. These amino acids are highlighted in green. Six orthologous sequences were aligned using the multiple sequence alignment program, Clustal Omega (see Web Resources). (B) Schematic representation of *OAS1* mutations. Black circles indicate the mutations in this study. Blue and red triangles indicate metal binding sites (p.Asp75,

p.Asp77, and p.Asp148) and ATP binding sites (p.Ser63, p.Lys213, and p.Gln229), respectively. Green and yellow boxes show the nucleotidyltransferase (NTP_transf_2) domain and 2',5'-oligoadenylate synthetase 1, domain 2, and C-terminus (OAS1_C) domain, respectively, predicted using the SMART program (see Web Resources).

Figure 3. Impact of the identified variations on protein structure

(A) Mapping of the mutations on the crystal structures of a double-stranded RNA (dsRNA)-bound form of human oligoadenylate synthetase 1 (hOAS1) and an apo form of porcine OAS1 (pOAS1) (PDB codes 4ig8 and 1px5, respectively).[22,23] The superimposed structures of the dsRNA-bound (cyan) and apo (green) forms of OAS1 are presented as ribbon diagrams. The stick model is shown in gray. The mutated residues are shown as van der Waals spheres in blue and dark green in the dsRNA-bound and apo forms, respectively. The substrate analog, 2'-deoxy ATP (dATP), and magnesium ions are shown as orange sticks and purple balls, respectively. Close-up views around the mutation sites are shown separately for the dsRNA-bound and apo forms. In the close-up views, some side chains of the hydrophobic residues

around the mutation sites are shown as translucent spheres.

(B) The free energy changes associated with each mutation in a dsRNA-bound form of hOAS1 and apo form of pOAS1 by the FoldX software are shown.[24]

Table 1. Demographic characteristics of five affected individuals in this study

	A-II-1	A-II-3	A-II-4	B-II-1	C-II-1
Consanguineous parents	No	No	No	No	No
Gestation (weeks)	38	36	39	39	39
Birth weight (g)	2,896	2,852	2,290	2,140	3,410
Gender	Male	Male	Female	Female	Female
Age at HSCT	Not done	151 d	Not done	8 m	11 m
Diagnosis of PAP	AU	BAL+AU	BAL+AU	BAL	BAL
Recurrent infection with hyperreactivity	Unknown	Unknown	Yes	Yes	Yes

Hypogammaglobulinemia	Unknown	Unknown	Yes	Yes	Yes
Leukocytosis with normal distribution	Yes	Yes	Yes	Yes	Yes
Splenomegaly before treatment	Yes	Yes	Yes	Unclear	Yes
Small and non-foamy AMs	Yes	Yes	Yes	Unclear	Yes
Respiration status					
Age at onset of respiratory dysfunction	39 d	39 d	49 d	2 m	5 m
Respiration status at birth	Well	Well	Well	Well	Well
Respiration status after BAL	Not done	Unchanged	Unchanged	Improved	Unchanged
Respiration status after IVIG	Unknown	Unknown	Improved	Improved	Improved
Outcome	Dead/91 d	Dead/163 d	Dead/11 y	Dead/3 y	Alive/19 m

Cause of death	Respiratory failure	Respiratory failure	Respiratory failure	Renal failure	Alive

AU, autopsy; BAL, bronchoalveolar lavage; HSCT, hematopoietic stem cell transplantation; d, day; m, month; y, year

Table 2. List of *OAS1* mutations detected in 3 unrelated families with GPAP

Variants	Prediction software			Grantham score
	SIFT	PolyPhen-2	MutationTaster	
c.227C>T, p.Ala76Val	0.08 (Tolerated)	0.936 (Probably damaging)	Polymorphism	64
c.326G>A, p.Cys109Tyr	0.18 (Tolerated)	0.715 (Possibly damaging)	Polymorphism	194
c.592C>G, p.Leu198Val	1.00 (Tolerated)	0.349 (Benign)	Polymorphism	32

*The cDNA position was based on RefSeq NM_01681

Web Resources

The URLs for data presented here are as follows:

Online Mendelian Inheritance in Man (OMIM), http://www.omim.org/

dbSNP, http://www.ncbi.nlm.nih.gov/projects/SNP/

NHLBI Exome Sequencing Project (ESP) Exome Variant Server,

http://evs.gs.washington.edu/EVS/

RefSeq, http://www.ncbi.nlm.nih.gov/RefSeq

Integrative Genomic Viewer, https://www.broadinstitute.org/igv

Exome Aggregation Consortium, http://exac.broadinstitute.org/

Human Genetic Variation Database, http://www.genome.med.kyoto-u.ac.jp/SnpDB/

SIFT, http://sift.jcvi.org

PolyPhen-2, http://genetics.bwh.harvard.edu/pph2

MutationTaster, http://www.mutationtaster.org

Multiple sequence alignment program, http://www.ebi.ac.uk/Tools/msa/clustalo/

SMART program, http://smart.embl-heidelberg.de/

References

1. Jobe, A.H. (1993). Pulmonary surfactant therapy. N. Engl. J. Med. *328*, 861–868.

2. Whitsett, J.A., Weaver, T.E. (2002). Hydrophobic surfactant proteins in lung function and disease. N. Engl. J. Med. *347*, 2141–2148.

3. Fitzgerald ML, X.R., Haley KJ, Welti R, Goss JL, Brown CE, Zhuang DZ, Bell SA, Lu N, McKee M, Seed B, Freeman MW. (2007). ABCA3 inactivation in mice causes respiratory failure, loss of pulmonary surfactant, and depletion of lung phosphatidylglycerol. J. Lipid Res. *48*, 621–632.

4. Uchida K, N.K., Trapnell BC, Terakawa T, Hamano E, Mikami A, Matsushita I, Seymour JF, Oh-Eda M, Ishige I, Eishi Y, Kitamura T, Yamada Y, Hanaoka K, Keicho N. (2004). High-affinity autoantibodies specifically eliminate granulocyte-macrophage colony-stimulating factor activity in the lungs of patients with idiopathic pulmonary alveolar proteinosis. Blood 103, 1089-1098.

5. Trapnell, B.C., Whitsett, J.A., Nakata, K. (.2003). Pulmonary alveolar proteinosis. N. Engl. J. Med. *349*, 2527–2539.

6. Uchida, K., Nakata, K., Carey, B., Chalk, C., Suzuki, T., Sakagami, T., Koch, D.E., Stevens, C., Inoue, Y., Yamada, Y., et al. (2014). Standardized serum GM-CSF autoantibody testing for the routine

clinical diagnosis of autoimmune pulmonary alveolar proteinosis. J. Immunol. Methods. *402*, 57–70.

7. Tazawa R, H.E., Arai T, Ohta H, Ishimoto O, Uchida K, Watanabe M, Saito J, Takeshita M, Hirabayashi Y, Ishige I, Eishi Y, Hagiwara K, Ebina M, Inoue Y, Nakata K, Nukiwa T. (2005). Granulocyte-macrophage colony–stimulating factor and lung immunity in pulmonary alveolar proteinosis. Am. J. Respir. Crit. Care Med. *171*, 1142–1149.

8. Handa, T., Nakatsue, T., Baba, M., Takada, T., Nakata, K., Ishii, H. (2014). Clinical features of three cases with pulmonary alveolar proteinosis secondary to myelodysplastic syndrome developed during the course of Behcet's disease. Respir. Investig. *52*, 75–79.

9. Hamvas, A., Cole, F.S., Nogee, L.M. (2007). Genetic disorders of surfactant proteins. Neonatology. *91*, 311–317.

10. Spagnolo, P., Bush, A. (2016). Interstitial lung disease in children younger than 2 years. Pediatrics. *1376*, e20152725.

11. Nogee, L.M., Garnier, G., Dietz, H.C., Singer, L., Murphy, A.M., deMello, D.E., Colten, H.R. (1994). A mutation in the surfactant protein B gene responsible for fatal neonatal respiratory disease in multiple kindreds. J. Clin. Invest. *93*, 1860–1863.

12. Nogee, L.M., Dunbar, A.E.r., Wert, S.E., Askin, F., Hamvas, A., Whitsett, J.A. (2001). A mutation in the surfactant protein C gene

associated with familial interstitial lung disease. N. Engl. J. Med. *344*, 73–79.

13. Tredano, M., Griese, M., Brasch, F., Schumacher, S., de Blic, J., Marque, S., Houdayer, C., Elion, J., Couderc, R., Bahuau, M. (2004). Mutation of SFTPC in infantile pulmonary alveolar proteinosis with or without fibrosing lung disease. Am. J. Med. Genet. A *126A*, 18–26.
14. Wambach, J.A., Casey, A.M., Fishman, M.P., Wegner, D.J., Wert, S.E., Cole, F.S., Hamvas, A., Nogee, L.M. (2014). Genotype-phenotype correlations for infants and children with ABCA3 deficiency. Am. J. Respir. Crit. Care. Med. *189*, 1538–1543.
15. Suzuki, T., Sakagami, T., Rubin, B.K., Nogee, L.M., Wood, R.E., Zimmerman, S.L., Smolarek, T., Dishop, M.K., Wert, S.E., Whitsett, J.A., et al. (2008). Familial pulmonary alveolar proteinosis caused by mutations inCSF2RA. J. Exp. Med. *205*, 2703–2710.
16. Suzuki, T., Trapnell, B.C. (2016). Pulmonary alveolar proteinosis syndrome. *Clin. Chest Med. 37*, 431–440.
17. Tanaka, T., Motoi, N., Tsuchihashi, Y., Tazawa, R., Kaneko, C., Nei, T., Yamamoto, T., Hayashi, T., Tagawa, T., Nagayasu, T., et al. (2011). Adult-onset hereditary pulmonary alveolar proteinosis caused by a single-base deletion in CSF2RB. J. Med. Genet. *48*, 205–209.
18. Hsu, A.P., McReynolds, L.J., Holland, S.M. (2015). GATA2 deficiency. Curr. Opin. Allergy Clin. Immunol. *15*, 104–109.

19. Imagawa, E., Osaka, H., Yamashita, A., Shiina, M., Takahashi, E., Sugie, H., Nakashima, M., Tsurusak, i.Y., Saitsu, H., Ogata, K., et al. (2014). A hemizygous GYG2 mutation and Leigh syndrome: a possible link? Hum. Genet. *133*, 225–234.

20. Yamada M, O.Y., Suzuki Y, Fukumura S, Miyazaki T, Ikeda T, Takezaki S, Kawamura N, Kobayashi I, Ariga T. (2012). Somatic mosaicism in two unrelated patients with X-linked chronic granulomatous disease characterized by the presence of a small population of normal cells. Gene. *497*, 110–115.

21. Van Durme, J., Delgado, J., Stricher, F., Serrano, L., Schymkowitz, J., Rousseau, F. (2011). A graphical interface for the FoldX forcefield. Bioinformatics. *27*, 1711–1712.

22. Hartmann, R., Justesen, J., Sarkar, S.N., Sen, G.C., Yee, V.C. (2003). Crystal structure of the 2'-specific and double-stranded RNA-activated interferon-induced antiviral protein 2“-5”-oligoadenylate synthetase. Mol. Cell. *12*, 1173–1185

23. Donovan, J., Dufner, M., Korennykh, A. (2013). Structural basis for cytosolic double-stranded RNA surveillance by human oligoadenylate synthetase 1. Proc. Natl. Acad. Sci. U. S. A. *110*, 1652–1657.

24. Schymkowitz, J., Borg, J., Stricher, F., Nys, R., Rousseau, F., Serrano, L. (2005). The FoldX web server: an online force field. Nucleic Acids Res. *33*, W382–388.

25. Justesen, J., Hartmann, R., Kjeldgaard, N.O. (2000). Gene structure and function of the 2'-5'-oligoadenylate synthetase family. Cell. Mol. Life Sci. *57*, 1593–1612.

26. Hamano, E., Hijikata, M., Itoyama, S., Quy, T., Phi, N.C., Long, H.T., Ha, L.D., Ban, V.V., Matsushita, I., Yanai, H., et al. (2005). Polymorphisms of interferon-inducible genes OAS-1 and MxA associated with SARS in the Vietnamese population. Biochem. Biophys. Res. Commun. *329*, 1234–1239.

27. He, J., Feng, D., de Vlas, S.J., Wang, H., Fontanet, A., Zhang, P., Plancoulaine, S., Tang, F., Zhan, L., Yang, H., et al. (2006). Association of SARS susceptibility with single nucleic acid polymorphisms of OAS1 and MxA genes: a case-control study. BMC Infect. Dis. *6*, 106.

28. Mashimo, T., Simon-Chazottes, D., Guénet, J.L. (2008). Innate resistance to flavivirus infections and the functions of 2'-5' oligoadenylate synthetases. Curr. Top. Microbiol. Immunol. *321*, 85–100.

29. Simon-Loriere, E., Lin, R.J., Kalayanarooj, S.M., Chuansumrit, A., Casademont, I., Lin, S.Y., Yu, H.P., Lert-Itthiporn, W., Chaiyaratana, W., Tangthawornchaikul, N., et al. (2015). High anti-dengue virus activity of the OAS gene family is associated with increased severity of dengue. J. Infect. Dis. *212*, 2011–2020.

30. Kosmider, B., Messier, E.M., Janssen, W.J., Nahreini, P., Wang, J., Hartshorn, K.L., Mason, R.J. (2012). Nrf2 protects human alveolar epithelial cells against injury induced by influenza A virus. Respir. Res. *13*, 43.

31. Golde, D.W. (1979). Alveolar proteinosis and the overfed macrophage. Chest. *76*, 119–120.

32. Mukae, H., Ishimoto, H., Yanagi, S., Ishii, H., Nakayama, S., Ashitani, J., Nakazato, M., Kohno, S. (2007). Elevated BALF concentrations of alpha- and beta-defensins in patients with pulmonary alveolar proteinosis. Respir. Med. *101*, 715–721.

33. Chang A, H.S., Kowalewska J, Flowers ME, Aneja T, Smith KD, Meehan SM, Nicosia RF, Alpers CE. (2007). Spectrum of renal pathology in hematopoietic cell transplantation: a series of 20 patients and review of the literature. Clin. J. Am. Soc. Nephrol. *2*, 1014–1023.

34. Palomar, L.M., Nogee, L.M., Sweet, S.C., Huddleston, C.B., Cole, F.S., Hamvas, A. (2006). Long-term outcomes after infant lung transplantation for surfactant protein B deficiency related to other causes of respiratory failure. J. Pediatr. *149*, 548–553.

35. Lachmann, N., Happle, C., Ackermann, M., Luttge, D., Wetzke, M., Merkert, S., Hetzel, M., Kensah, G., Jara-Avaca, M., Mucci, A., et al. (2014). Gene correction of human induced pluripotent stem cells repairs the cellular phenotype in pulmonary alveolar proteinosis.

Am. J. Respir. Crit. Care. Med. *189*, 167–182.

36. Nakata, K., Gotoh, H., Watanabe, J., Uetake, T., Komuro, I., Yuasa, K., Watanabe, S., Ieki, R., Sakamaki, H., Akiyama, H., et al. (1999). Augmented proliferation of human alveolar macrophages after allogeneic bone marrow transplantation. Blood. *93(2)*, 667–673.

37. Suzuki, T., Arumugam, P., Sakagami, T., Lachmann, N., Chalk, C., Sallese, A., Abe, S., Trapnell, C., Carey, B., Moritz, T., et al. (2014). Pulmonary macrophage transplantation therapy. Nature. *514*, 450–454.

Fig. 1

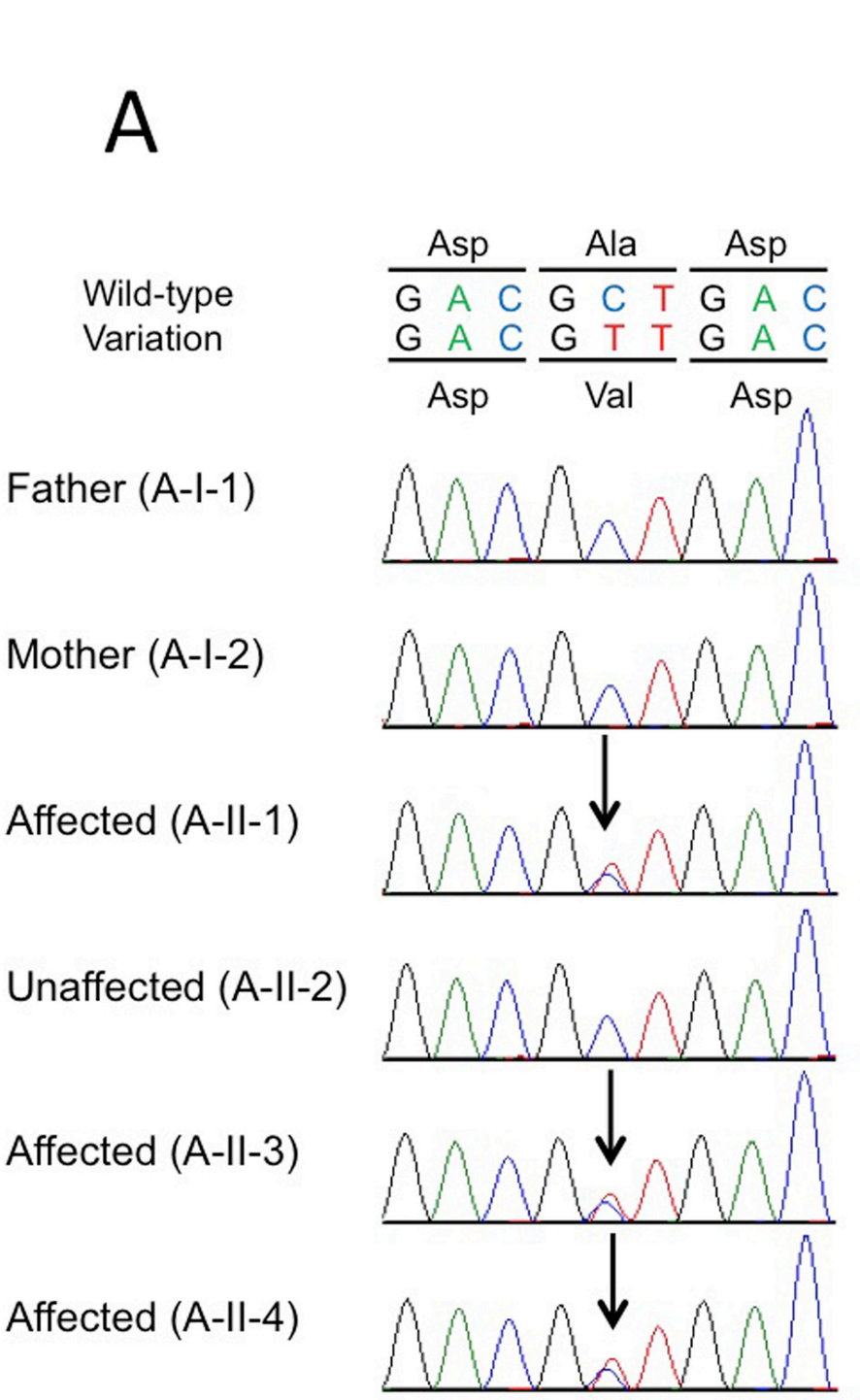
A
Asp Ala Asp
Wild-type G A C G C T G A C
Variation G A C G T T G A C
Asp Val Asp
Father (A-I-1)
Mother (A-I-2)
Affected (A-II-1)
Unaffected (A-II-2)
Affected (A-II-3)
Affected (A-II-4)

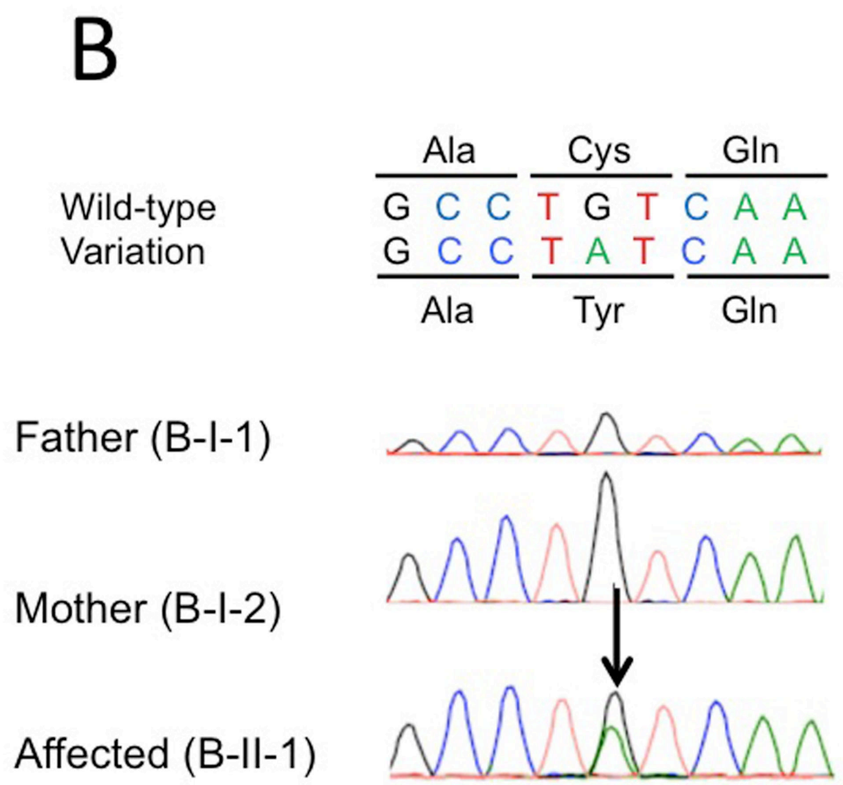
B
Ala Cys Gln
Wild-type G C C T G T C A A
Variation G C C T A T C A A
Ala Tyr Gln
Father (B-I-1)
Mother (B-I-2)
Affected (B-II-1)

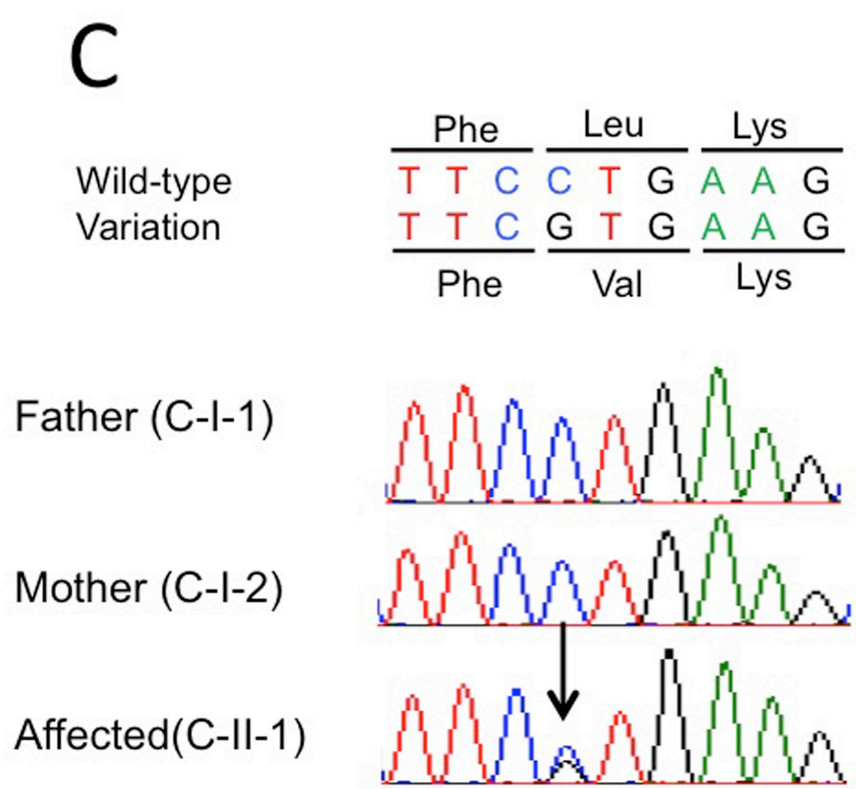
C
Phe Leu Lys
Wild-type T T C C T G A A G
Variation T T C G T G A A G
Phe Val Lys
Father (C-I-1)
Mother (C-I-2)
Affected(C-II-1)

Fig. 2

A

	p.76	p.109	p.198
Human OAS1 (NP_058132.2)	71 RGRSDADLVVF 81	104 RQLEACQRERA 114	193 LQRDFLKQRPT 203
Rhesus OAS1 (NP_001077418.1)	71 RGRSDADLVVF 81	104 KQLEACQRERA 114	193 LQRNFLKQRPT 203
Mouse Oas1a (NP_660212.2)	72 KGKSDADLVVF 82	105 KQLYEVQHERR 115	194 LQRNFLKQRPT 204
Mouse Oas1g (NP_035982.2)	72 KGRSDADLVVF 82	105 KQLYEVQHERR 115	194 LQRNFLKQRPT 204
Dog OAS1 (NP_001041596.1)	71 RGRSDADLVVF 81	104 RQLEACQREET 114	193 LQRDFLRQRPT 203
Elephant OAS1 (XP_010597265.1)	68 KGRSDADLVVF 78	101 KQLEACQREEE 111	186 LQRAFLKQRPT 196
Opossum OAS1 (XP_001378808.3)	74 RGLSDADLVVF 84	107 KQLEACQHEQG 117	195 LQKRFLKERVT 205

B

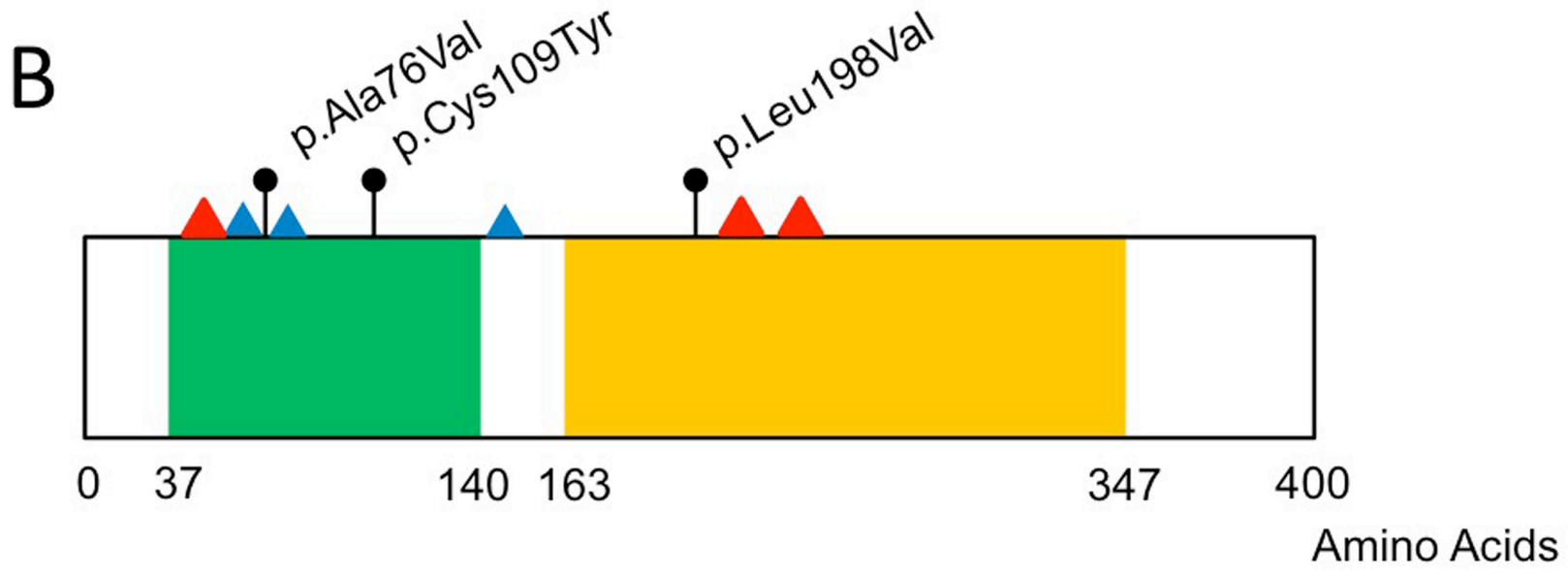

Fig. 3

A

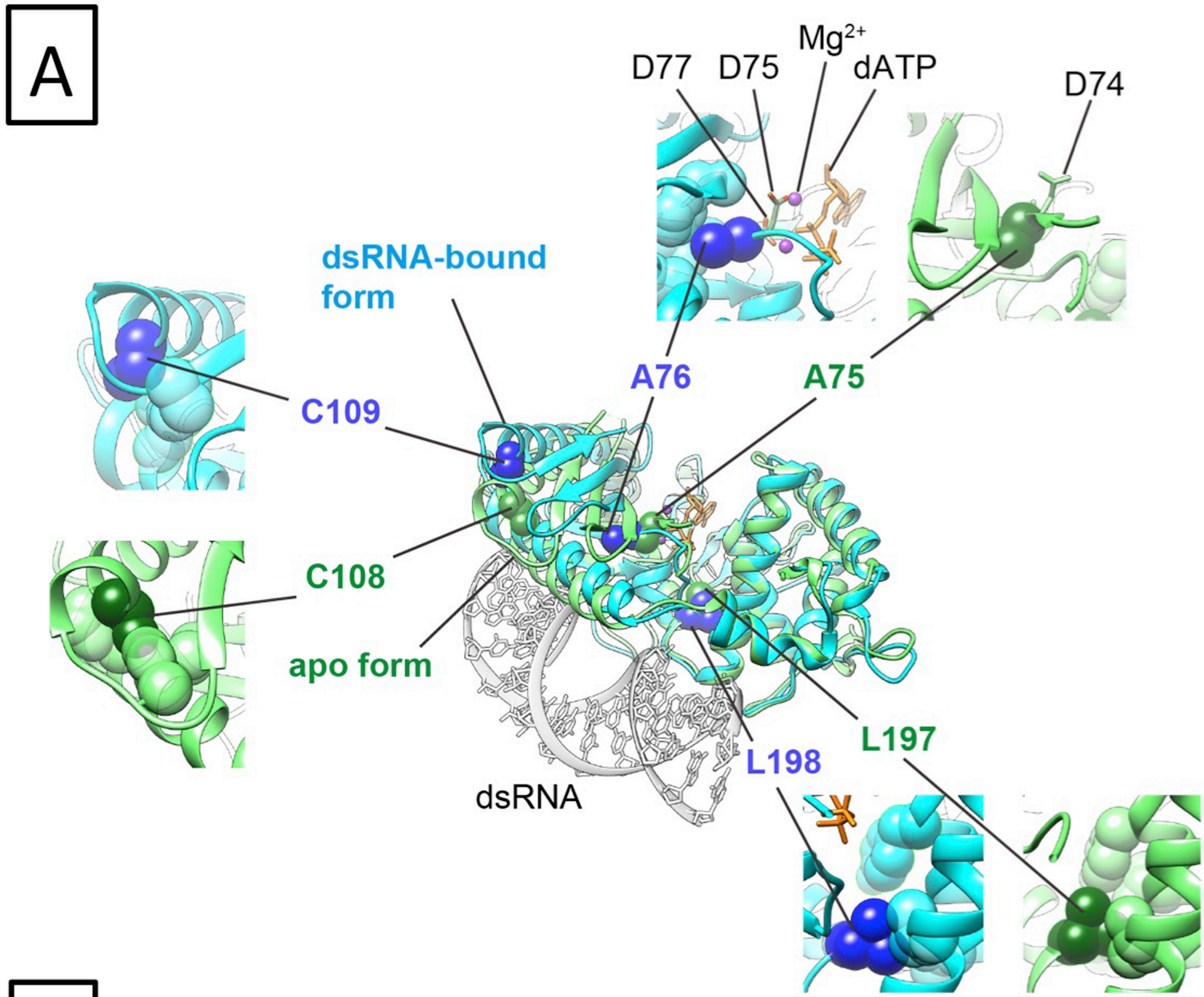
D77
D75
Mg2+
dATP
D74
dsRNA-bound form
A76
A75
C109
C108
apo form
L197
L198
dsRNA

B

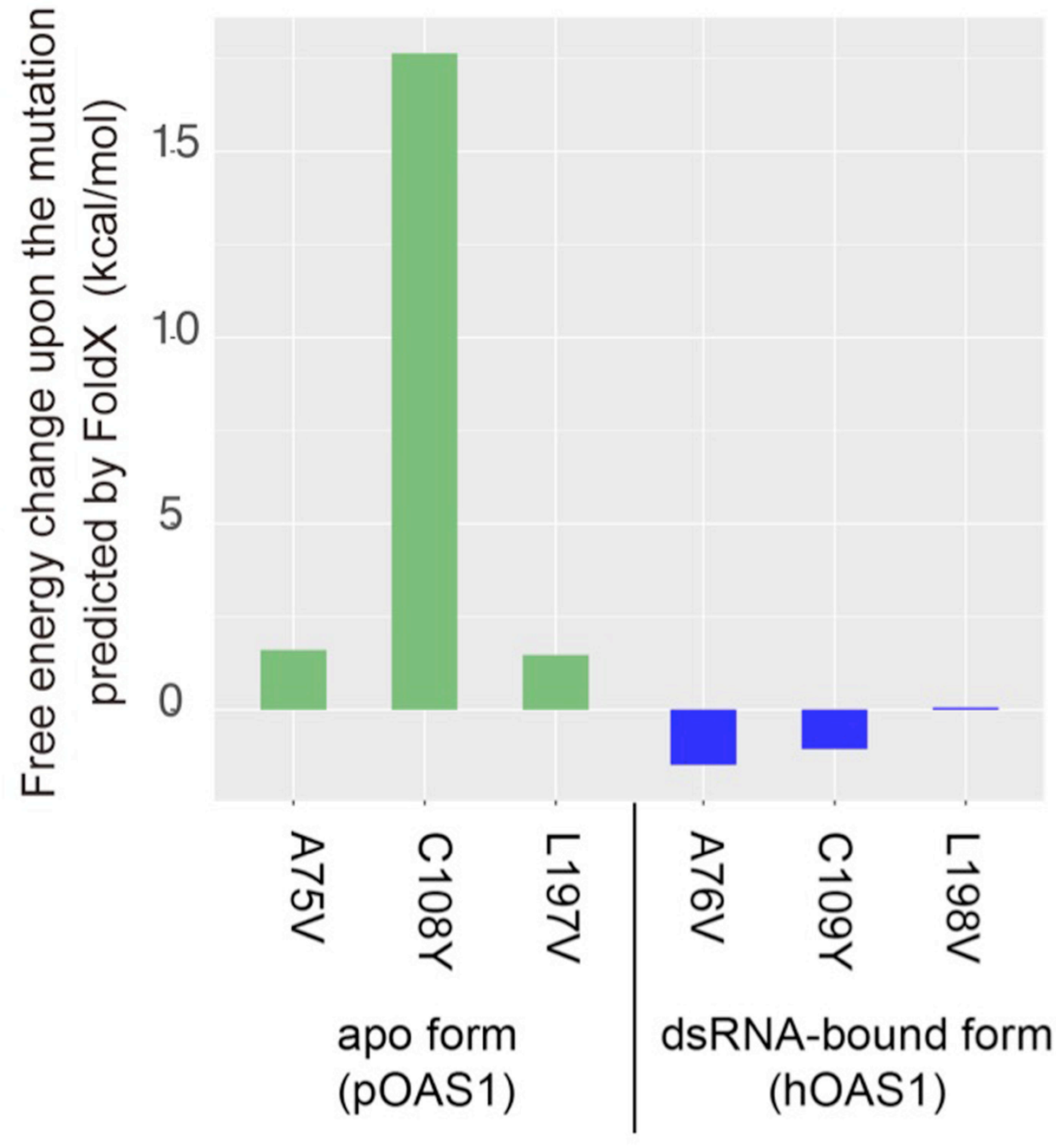
Free energy change upon the mutation predicted by FoldX (kcal/mol)
1.5
1.0
.5
0
A75V
C108Y
L197V
A76V
C109Y
L198V
apo form (pOAS1)
dsRNA-bound form (hOAS1)